
LASER
SPECTROSCOPY

Measurement of the Hot Zone Temperature Using 1f Modulation Diode Laser Absorption Spectroscopy with Logarithmic Signal Conversion

V. V. Liger^a, V. R. Mironenko^a, Yu. A. Kuritsyn^a, and M. A. Bolshov^{a,*}

^a*Institute of Spectroscopy, Russian Academy of Sciences, Troitsk, Moscow, 108840 Russia*

^{*}*e-mail: bolshov@isan.troitsk.ru; mbolshov@mail.ru*

Received May 19, 2022; revised May 19, 2022; accepted May 19, 2022

Abstract—New version of diode laser (DL) absorption spectroscopy (DLAS) for determining the hot zone temperature is developed. The method is based on the combination of slow scanning of the radiation frequency of a probe DL around the absorption line of a test molecule of the medium and fast radiation frequency modulation with an amplitude on the order of the absorption line width. The developed version of the wavelength-modulation (WM-DLAS) is based on the two-beam differential scheme, the logarithmic signal conversion, and the registration of absorption at the first harmonic of the modulation frequency. The two-beam differential registration scheme and the logarithmic conversion of absorption signals have made it possible to reduce substantially the nonselective absorption of probe radiation and registration noise determined by excessive noise of lasers. The application of the first harmonic has ensured a higher sensitivity of the proposed version of WM-DLAS. Using the technique developed in this study, we have measured the temperature of water vapor in atmospheric air in the range 700–1100 K. The results are compared with the data obtained using commercial thermocouples. The difference in temperatures measured by a standard thermocouple and its mean value determined using the technique developed here is 40 K for a temperature of 1000 K and 30 K for 800 K.

Keywords: absorption spectroscopy, diode laser, temperature measurement

DOI: 10.3103/S1068335623130067

1. INTRODUCTION

At present, spectroscopic methods with diode lasers (DLs) are widely used for studying processes in gas mixtures of various types (atmosphere, flames, and multicomponent gas flows). In view of their relative simplicity and high sensitivity in the detection of atoms and molecules, the method of absorption spectroscopy with DLs (diode laser absorption spectroscopy, DLAS) has been developed most comprehensively. This method is widely used for contactless detection of main components of air (H₂O, CO, CO₂, CH₄, etc.) [1–8]. In hot zones, the DLAS method makes it possible to measure the temperature, the total pressure of gas mixtures, and the partial pressures of main molecular components with a time resolution in micro- and millisecond ranges [9–12]. The main advantages of the DLAS method include its relative simplicity, comparatively low cost of basic components, and the possibility of delivering DL probe radiation to a hot zone via an optical fiber. The latter factor makes it possible to arrange the sensitive detecting part of the DLAS sensor far from the hot zone with high acoustic and electric noise [13].

The method for determining the temperature of a medium using DLAS is based on measuring the integral absorption at several lines of a test molecule, which have different lower levels of transitions [14]. In turn, the integral intensities of absorption lines are determined by fitting the experimental spectrum by the model spectrum constructed using spectroscopic databases. Having determined the temperature of the medium in this way, it is possible to find the concentrations of molecular components of the mixture from the absorption of DL probe radiation at the optical length in the object.

By now, various versions of DLAS have been developed for determining the temperature of the medium, which are based on direct absorption spectroscopy (DAS) as well as several versions of spectroscopy with modulation of the wavelength of the probing DL (wavelength-modulation spectroscopy, WMS). The DAS method for determining the parameters of a medium is the simplest [15–17].

This method operates well when the fluctuations of the base line (BL) are not very strong as compared to the absorption signal so that the integral intensity of the absorption line can be determined with an acceptable accuracy. In the opposite case of a low line intensity, BL variations substantially reduce the accuracy in determining temperature. Such a situation is typical in the case of a high turbulence in the gas zone, the instability of DL radiation and detecting systems, as well as for a high level of irradiation of the detector by broadband radiation of the hot zone being probed.

In WMS, the influence of noise on the accuracy of determining the intensities of absorption lines is substantially lower [18, 19]. In this method, apart from a slow scanning of the DL wavelength within the tuning range (with frequencies $f \sim 1$ kHz), fast modulation of the wavelength is performed in the limits comparable with the absorption line width and with frequencies $f \sim 10\text{--}100$ kHz. A useful absorption signal is detected at harmonics kf using synchronous detection. In this case, a low-frequency flicker noise is suppressed, and the signal/noise ratio increases (i.e., the MS sensitivity is higher than the DAS sensitivity). This is important when DLAS is used for diagnostics of turbulent hot zones of the type of internal combustion chambers, hot exhausts of jet engines, and combustion processes in gas flows.

A serious disadvantage of first WMS versions was the required calibration of the systems for each specific realization of the sensor. This difficulty has been overcome in the next WMS versions. Systems that do not require calibration (calibration-free wavelength modulation spectrometry, CF-WMS) have been developed [20–23]. In view of the absence of a generally accepted term for this method, it will be referred here as calibration-free WMS. Most often, normalization of absorption signal harmonics kf/nf (usually $2f/1f$) is used. The combination of the normalization with the processing of absorption signals with account of DL tuning characteristics makes it possible to determine the hot zone parameters without calibration of the sensor using the measurements in a cell containing a gas mixture with known composition and parameters. In any version of the WMS method, it is necessary to determine preliminarily and exactly the tuning and modulation characteristic of the DL used for obtaining information on the parameters of the gas being tested. It should be noted that the algorithms for processing the data in the MS method are also much more complicated as compared to the DAS method.

One of radical methods for eliminating the dependence of the output signal of the sensor on nonselective variations of the intensity of laser radiation being detected is the use of a scheme with logarithmic signal conversion. Several techniques for the application of LC together with WMS-DLAS was described in the literature. In [24, 25], the LC of signals in detecting chlorine atoms in a glow discharge enabled researchers to suppress excessive laser noise. In [26], the ability of a logarithmic scheme to ensure a large dynamic range of the output signal linearity was demonstrated. The CF-WMS method including the combination of WMS with LC was used for determining the concentration of absorbing molecules [27–30]. However, in all publications, the second harmonics was detected at a relatively low modulation frequency of the laser radiation wavelength, and isolated absorption lines were measured.

In our earlier publication [31], we proposed a version of the CF-WMS method using a combination of the LC of experimental data and MS with the registration of the first harmonics of the absorption signal of a test molecule. The proposed version of DLAS and the processing algorithm substantially simplify the experimental data processing as compared to other versions of CF-WMS. The method proposed in [31] was employed for determining the integral intensity of a single absorption line of the H_2O molecule at the atmospheric pressure and room temperature.

In this study, we investigate the possibility of application of the method proposed in [31] for determining the hot zone temperature by measuring the first harmonics of the signals for two absorption lines of a test molecule. We have used two DLs emitting in the range $1.3\text{--}1.4\ \mu\text{m}$. The radiation wavelengths of the lasers were alternatively scanned in the absorption region of the chosen H_2O line (temporal multiplexing) with a frequency of 122 Hz. The DL wavelengths were modulated simultaneously with a frequency of ~ 50 kHz. In the data detection and processing system, we used the LC of the signals from both lasers, the differential scheme of registration, and synchronous detection, which made it possible to reduce substantially the noise level and the influence of background.

2. THEORETICAL FOUNDATION OF THE METHOD

The absorption of light is described by the Bouguer–Lambert–Beer law

$$\frac{I_t}{I_0} = \exp[-\alpha(\nu)] = \exp\left[-\sum_j \int_0^L S_j(T) N_j g_j(\nu) dl\right], \quad (1)$$

where I_t is the laser radiation intensity after the passage through an absorbing medium of length L [cm]; I_0 is the intensity of laser radiation; $\alpha(\nu)$ is the dimensionless absorption coefficient; ν is the laser radiation frequency; $S_j(T)$ [cm/mol] is the intensity of the j th transition; N_j [mol/cm³] is the concentration of the test molecules; and $g_j(\nu)$ [cm] is a function describing the absorption line-shape that depends on the temperature, pressure, and composition of the gas mixture and is determined by the mechanisms of its broadening.

The line intensity is a function of temperature and is described with admissible accuracy by expression

$$S(T) \approx S(T_0) \frac{Q(T_0)}{Q(T)} \exp \left[-\frac{hcE''}{k} \left(\frac{1}{T} - \frac{1}{T_0} \right) \right], \quad (2)$$

where T_0 is reference temperature; $Q(T)$ is the statistical sum that depends only on temperature; h is the Planck constant; c is the velocity of light; E'' is the energy of the lower state of transition, and k is the Boltzmann constant. Since the integral of $g(\nu)$ equals unity by definition, integral absorption A_j [cm⁻¹] at an individual transition in a homogeneous medium can be expressed as

$$A_j(T) = \int_{-\infty}^{\infty} \alpha_j(\nu) d\nu = \int_0^L S_j(T) N dl = S_j(T) NL. \quad (3)$$

The gas temperature can be determined by measuring absorption at two different wavelengths corresponding to different energies of the lower level of the transition. In this case, ratio R of integral absorptions for a homogeneous medium, which is a function of temperature and is independent of concentration N and length L , is given by

$$A = \frac{A_2}{A_1} = \frac{S_2(T)}{S_1(T)}. \quad (4)$$

Therefore, to measure the gas temperature, it is sufficient to measure the integral intensities of the absorption lines for two transitions. Expression (3) shows that to determine integral intensity A_j of a line, it is necessary to measure its spectral line-shape $g_j(\nu)$. In actual situations, for determining $g_j(\nu)$, the fitting of the experimental data not only by an isolated contour, but also by spectral intervals in the vicinity of the chosen lines is used.

The errors in temperature measurements usually depend on the accuracy of the measurement of DL probe radiation parameters and on the accuracy of determining the line-shapes. In actual industrial facilities and experimental setups, there are many factors limiting these accuracies. These issues will be considered below in the description of the measuring technique and data processing.

In this study, we propose the differential scheme with wavelength (optical frequency) modulation of DL radiation, logarithmic conversion of photosignals, and the registration of the first harmonics of absorption signals to minimize the error in determining temperature [31].

Let us consider the operation principle of such a scheme. The main fraction of DL radiation through a single-mode fiber in the sample channel is delivered to the test object. A part of radiation is directed to the reference channel that does not contain the absorbing medium. The signals from photodetectors of the sample and reference channels are delivered to the logarithmic converter and then to the differential amplifier. The absorption is detected using a synchronous detector at the first harmonic of the DL wavelength modulation frequency. Assuming that photodiodes operate in the linear region of the dynamic range, photocurrent i_s in the sample channel can be written as

$$i_s(t) = G_s [I_0(t) \tau_s(t) \tau_{vs}(t) \exp(-\alpha) + E(t)] + i_{\text{noise}}, \quad (5)$$

where G_s is the watt–ampere responsivity of the photodiode; $I_0(t)$ is the DL radiation intensity; $\tau_s(t)$ and $\tau_{vs}(t)$ are the frequency-dependent and independent components of the transmission coefficient of the sample channel (τ_{vs} is determined as a rule by the interference effects and does not include absorption by molecules); $E(t)$ is the intensity of broadband radiation incident on the photodiode; and i_{noise} are the noise sources that are not associated with radiation in the sample channel.

It can be seen from expression (5) that the intensities of laser and broadband radiations, as well as uncertainties and instability of the transmission coefficient, affect the accuracy of measurement of the absorption coefficient. For high laser radiation intensities and for appropriate spectral and spatial filtrations, the effect of the noise current and broadband radiation can be ignored. This simplifies expression (5):

$$i_s = G_s [I_0(t) \tau_s(t) \tau_{vs}(t) \exp(-\alpha)]. \quad (6)$$

An analogous expression can be written for the reference channel, in which selective absorption is absent:

$$i_r = G_r[I_0(t)\tau_r(t)\tau_{vr}(t)]. \quad (7)$$

After passing signals through the logarithmic converter, the voltages at the outputs of the sample and reference channels are

$$U_s = K\{\ln G_s + \ln \tau_s + \ln \tau_{vs} + \ln[I_0(t)] - \alpha\}, \quad (8)$$

$$U_r = K\{\ln G_r + \ln \tau_r + \ln \tau_{vr} + \ln[I_0(t)]\}, \quad (9)$$

where K is the logarithmic conversion coefficient. After subtraction, the voltage at the output of the differential amplifier is

$$U_{\text{dif}} = K\left(\ln \frac{G_r}{G_s} + \ln \frac{\tau_r}{\tau_s} + \ln \frac{\tau_{vr}}{\tau_{vs}}\right) + K\alpha. \quad (10)$$

The first term in the parentheses is a constant, while the second term fluctuates with characteristic frequencies that normally range from zero to several tens of kilohertz. For the sensor design developed for our experiments, the third term associated with interference noise is reduced significantly [31]. Therefore, if the absorption coefficient is modulated at frequencies of several tens of kilohertz and higher, the output signal from the LC at the modulation frequency becomes proportional to the absorption coefficient.

The DL radiation frequency is modulated by varying the injection current. The DL radiation frequency increases (or decreases) upon a change of this current; for this reason, for a periodic scanning of the absorption line profile, the laser is pumped by a saw-tooth or triangular current with a relatively low scanning frequency (hundreds or thousands of Herz). For modulation of the DL wavelength, a sinusoidal current of frequency f equal to several tens of kilohertz is added to the pumping current. Apart from radiation frequency modulation, modulation is performed for the radiation intensity, which can be written in this case in the form

$$I_0(t) = \bar{I}_0 + a \cos(2\pi ft + \psi_1) + b \cos(4\pi ft + \psi_2), \quad (11)$$

while the optical frequency can be written as

$$\nu = \bar{\nu} + m \cos(2\pi ft). \quad (12)$$

Here, \bar{I}_0 and $\bar{\nu}$ are the radiation intensity and optical frequency, which are averaged over the modulation period; a and b are the linear and nonlinear amplitudes of intensity modulation; ψ_1 and ψ_2 are the phase shifts of the signals modulating the optical frequency and the intensity for the first and second harmonics, respectively, and m is the amplitude of the optical frequency modulation.

Absorption coefficient α can be written in the form of Fourier series:

$$\alpha(\nu) = \alpha(\bar{\nu} + m \cos(2\pi ft)) = \sum_0^{\infty} H_n(\bar{\nu}, m) \cos(2\pi nft). \quad (13)$$

Here,

$$H_0(\bar{\nu}, m) = \frac{1}{2\pi} \int_{-\pi}^{\pi} \alpha(\bar{\nu} + m \cos \varphi) d\varphi; \quad (14)$$

$$H_n(\bar{\nu}, m) = \frac{1}{\pi} \int_{-\pi}^{\pi} \alpha(\bar{\nu} + m \cos \varphi) \cos(n\varphi) d\varphi; \quad n > 0. \quad (15)$$

The first harmonic of the output voltage takes the form

$$U_{\text{out},1f}(\bar{\nu}, m) = K \left[\ln \left(\frac{\tau_r}{\tau_s} \right)_{1f} + \ln \left(\frac{\tau_{vr}}{\tau_{vs}} \right)_{1f} \right] + KH_1(\bar{\nu}, m). \quad (16)$$

The term in the square brackets represented the base line. Since the base line and the absorption signal become additive after the logarithmic conversion, it becomes possible to separate them using the difference in their frequency characteristics.

In most technical applications, the noise spectrum lies in the low-frequency region. Synchronous detection at a laser modulation frequency noticeably exceeding the upper boundary of flicker noise makes

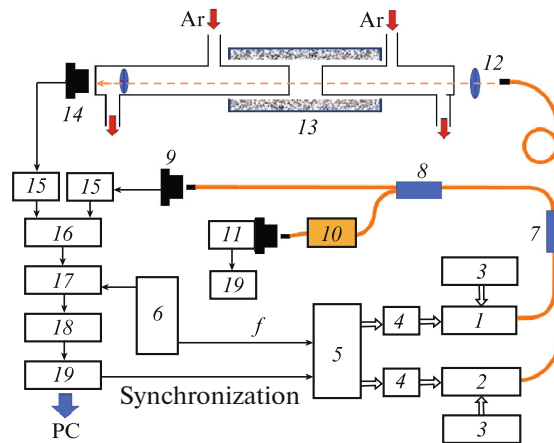


Fig. 1. Block diagram of experimental setup: (1, 2) laser diodes; (3) temperature controllers; (4) pumping current controllers; (5) saw-tooth voltage former; (6) sound generator; (7, 8) fiber-optical splitters; (9) reference channel photodiode; (10) Mach–Zehnder fiber-optical interferometer; (11) photodetector of the interferometric channel; (12) objective lens; (13) measuring cell with a tube furnace; (14) sample channel photodiode; (15) logarithmic converters; (16) differential amplifier; (17) synchronous detector; (18) lower-frequency filter; and (19) data collection system.

it possible to separate effectively the output signal component, which is proportional to the first harmonic of the absorption coefficient.

In this study, we used two DLs for determining the gas medium temperature because for a limited wavelength range of DL tuning, it is impossible to find the spectral region in which high-intensity absorption lines of water with noticeably different energies of the lower transition levels are located. When two lasers are used, the slow scanning parameters were selected for each laser to ensure the registration of the absorption lines that are optimal for determining the gas temperature. The modulation frequencies for both lasers were chosen identical. Directing radiations from the two lasers alternately into the sample channel, we obtained a sequence of spectral interval scans with alternating values of the first harmonics of the absorption coefficients for two H_2O lines at the synchronous detector outputs. These spectra were subsequently used for determining the gas temperature.

3. EXPERIMENT

3.1. Experimental Setup

To verify the method, we performed absorption temperature measurements for air containing water vapor. The schematic diagram of the experimental setup is shown in Fig. 1.

For measuring spectra, we used distributed feedback laser diodes 1 (NEL209042) and 2 (Zacher Lasertechnik 1343-05-BFY). The required temperature and injection current were maintained by controllers 3 (Thorlabs TED350) and 4 (Thorlabs LDC202), respectively. Scanning of the lasers in the required spectral interval was performed by varying the injection current using self-made saw-tooth voltage generator 5 operating at a frequency of 122 Hz. The wavelength modulation of DL radiation was performed by a sinusoidal current of frequency $f = 50$ kHz from generator 6 (Instek GFG-8219a), which was summed with the scanning current. For detecting signals in different spectral ranges, the laser worked alternately; the scan durations and modulation frequencies were identical for both lasers, but the amplitudes of the saw-tooth and sinusoidal current components were optimized individually for each laser.

Laser beams were superposed in the same single-modal fiber by fiber-optical splitter 7; then mixed radiation was split by the same splitter into two parts (50%/50%). A part of radiation (40%) was directed via splitter 8 to photodiode 9 of the reference channel. Other 10% of radiation were fed to the input of the interferometric channel consisting of a Mach–Zehnder fiber-optical interferometer 10 and photodetector 11 with a transmission band of 10 MHz. The interferometer included two fiber-optical splitters and a patch cord with a length of ~ 30 cm. The free spectral range of the interferometer was 0.012 cm^{-1} .

After the splitting in fiber-optical splitter 7, the main part of radiation (50%) was collimated by short-focus objective lens 12 (Thorlab F240APC-C) and was directed to measuring cell 13 consisting of a quartz tube furnace of length 30 cm with an inner diameter of 25 mm and two quartz inserts with outer diameters of 20 mm. The inserts were pushed into the furnace from two sides until they were separated by

a gap of length 8 cm approximately at the center of the tube furnace, where the temperature gradient was minimal. The inner end of each insert had a wedge-type quartz window, which reduced interference distortions of the signal. The opposite ends of the inserts had attachments for the input and output radiation in the cell. These attachments were also used for flushing the inner parts of the inserts with dried argon. This allowed us to localize the region containing water vapor inside the quasi-homogeneous region of the furnace. The temperature in this region was measured by K-type thermocouples at three points (at the center and at the edges). For the maximal heating to 1300 K, the temperature variation in the measuring volume did not exceed 8 K.

At the exit of the cell, radiation was focused by a lens ($F = 3$ cm) and registered by pin-photodiode *14* made of InGaAs (Hamamatsu). The signals from the sample and reference channels were fed to logarithmic converters *15* (based on assemblies of MAT-04 transistors and Analog Device AS 8034 operation amplifiers) and then subtracted and amplified by differential amplifier *16*. The difference signal was detected at modulation frequency f by self-made synchronous detector *17* designed based on an Analog Device AD633 multiplier. After filtration by low-frequency filter *18*, the signal was fed to the data collection and processing system (NI USB 6281 DAQ, National Instruments) and then to the computer.

3.2. Choice of Absorption Lines of the Test Molecule

The choice of the optimal lines from a set of H₂O lines in the near IR range was based on the search software [32] developed based on minimization of measuring errors δT of integral intensities A_j of the lines.

Explicit expression for quantity δT with account for relations (2) and (4) can be written in the form

$$\delta T = \frac{T^2}{T_{\text{eff}}} \left(\frac{1}{S_1^2} + \frac{1}{S_2^2} \right)^{1/2} \delta S, \quad (17)$$

where $T_{\text{eff}} = hc\Delta E/k$ and ΔE is the energy difference between the lower levels of two transitions in H₂O. In actual conditions, noise existing in the system leads to statistical errors in the measurements of integral intensities A_j of the lines. To estimate error δT , we assume that it is possible to detect a change in the absorption of 10^{-3} (0.1%) against the noise background. For an absorption line width of ~ 0.05 cm⁻¹, this corresponds to integral absorption $A_{\text{min}} \sim 5 \times 10^{-5}$ cm⁻¹.

The experimentally determined values of $A_j = S_j NL$ depend not only on S_j , but also on layer thickness L and vapor concentration N . The choice of the lines for measuring requires analysis of the $A_j(T)$ dependence in the range of temperatures being measured, i.e., the account for the temperature dependence of not only S_j , but also of water vapor concentration N . Since $A_{\text{min}} = \delta S NL$, we have $\delta S = A_{\text{min}}/NL$. For constant total pressure P and relative water vapor concentration χ , the expression for N takes form $N = \chi kT$, and error δT of temperature measurement can be expressed as

$$\delta T = \frac{kT^3}{T_{\text{eff}} P \chi L} \left(\frac{1}{S_1^2} + \frac{1}{S_2^2} \right)^{1/2} A_{\text{min}}. \quad (18)$$

For $T = 1000$ K, $P = 1$ atm, $\chi = 0.02$, and $L = 10$ cm, optimal integral absorption $A_{\text{min}} = 10^{-4}$ cm⁻¹ corresponds to $\delta S_x \sim 3.4 \times 10^{-23}$ cm/mol. For other temperatures, δS is determined from relation $\delta S = \delta S_x T/T_x$, and expression (18) takes form

$$\delta T = \frac{T^3}{T_{\text{eff}} T_x} \left(\frac{1}{S_1^2} + \frac{1}{S_2^2} \right)^{1/2} \delta S. \quad (19)$$

For a pressure of 1 atm, we have selected lines at frequencies of 7185.6 and 7466.34 cm⁻¹. For the chosen pair of lines and for given values of the statistical error, dependence $\delta T(T)$ is shown in Fig. 2.

3.3. Selection of Parameters for Scanning and Modulation of Lasers

The fundamental factor in temperature measurements is the transmission of radiation beams from both lasers through the same optical path. For this reason, in the sensor prototype proposed here, temporal multiplexing is used, and the signals from the two lasers are measured using the same detection system (DS) that consists of photodetector *14*, logarithmic converters *15*, differential amplifier *16*, and synchro-

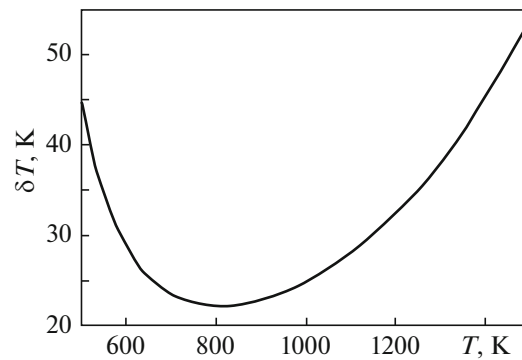


Fig. 2. Temperature dependence of statistical error δT of the cell temperature estimate on measuring T for lines 7185.6 and 7466.34 cm^{-1} .

nous detector 17 (see Fig. 1). It is important that the signals of the first derivatives of absorption lines of both lasers, get into the linear DS region.

First, the tuning of parameters of scanning and sinusoidal modulation of lasers was performed. Preliminary investigations have shown that laser characteristics differ significantly; for this reason, the amplitudes of the saw-tooth voltage and sinusoidal modulation amplitude were tuned separately.

First, the DLs were tuned by applying the saw-tooth voltage for measuring spectra near the chosen absorption lines (lasers 1 and 2 were tuned in the vicinity of frequencies 7185 cm^{-1} and 7466 cm^{-1} , respectively; henceforth, these lasers will be referred to as laser 7185 and laser 7466). Then we analyzed the modulation characteristics of the lasers in the chosen scanning ranges. The absolute value of the laser wavelength modulation was measured using the pattern of oscillations at the photodetector output in the interference channel. Figure 3a shows the dependences of modulation amplitude m of the optical frequency of the lasers on current modulation frequency f . It can be seen that for a fixed intensity modulation amplitude, the values of m decrease quite rapidly upon an increase in f from 45 to 1000 kHz. For this reason, all subsequent measurements were taken at frequency $f = 50$ kHz. Figure 3b shows the dependences of optical modulation amplitude m on laser current modulation amplitude for this frequency. It can be seen that in the measurement region, amplitudes m increase linearly with increasing current modulation amplitude. At the same time, laser 7466 is modulated much better than laser 7185 (for the same current modulation amplitude, the value of m for the former laser is three times larger).

The dependences of the amplitudes H_1 (peak-to-peak) of the first harmonic signals on optical frequency modulation amplitudes m are shown in Fig. 4. Since laser 7466 radiation line is weak, the modulation amplitude m_2 for this line has been established from the maximal signal of the first harmonic, which has been attained for $m_2 \sim 0.04 \text{ cm}^{-1}$. Conversely, for the strong line of laser 7185, modulation amplitude m_1 was reduced to make the first harmonic signals for both lines commensurate and located in the linear range of the registration system. The value of m_1 was chosen at $\sim 0.02 \text{ cm}^{-1}$. The experimentally established values of m_1 and m_2 were determined from the transmission spectrum of the interferometer.

3.4. Temperature Measurements

After the attainment and stabilization of the required temperature, argon flushing of quartz inserts was performed. Simultaneously, argon was flushed through the inner part of the furnace. Despite the prolonged (for several minutes) puffing, the photodiode of the sample channel registered the residual signal of water absorption near the line 7185 cm^{-1} , which is associated with the presence of small unflushed gaps in the cell and the residual concentration of water vapor in the high-purity argon tank. This signal was recorded as a background signal and was subsequently used in processing of the results of measurements. Then the argon flow through the inner part of the oven was discontinued, and this part was filled with atmospheric air saturated with water vapor at room temperature. After the temperature stabilization, the signal was registered.

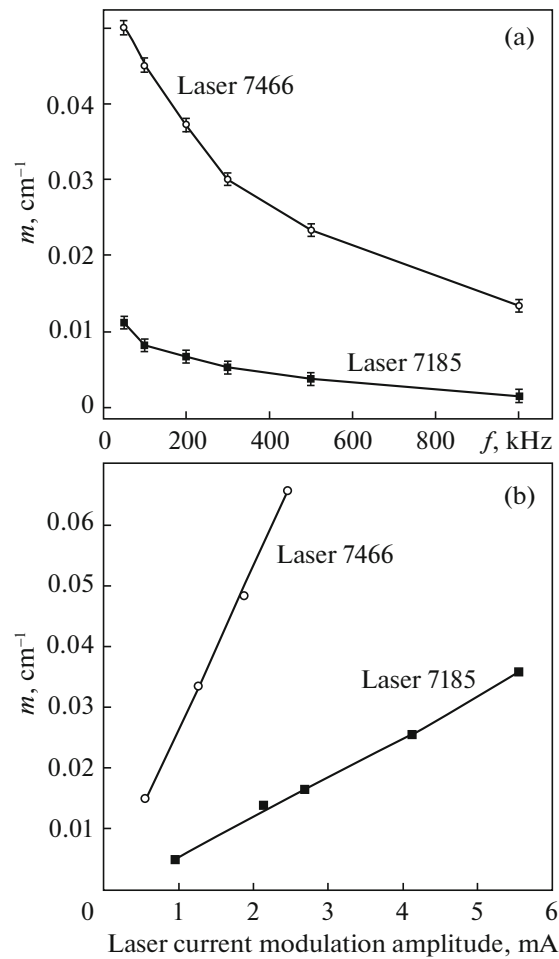


Fig. 3. Dependences of modulation amplitudes m of the laser optical frequency on modulation frequency f for fixed current modulation amplitudes (a) and on the current modulation frequency at a frequency of 50 kHz (b).

4. PROCESSING OF SPECTRA AND RESULTS

We recorded spectra at temperatures in the range 700–1100 K. Optical frequency modulation amplitudes m_1 and m_2 were set at 0.0195 and 0.0342 cm^{-1} , respectively. At each temperature, 18 scans were registered in each measurement. The scans were summed, and fitting to theoretical spectrum $H_1(\bar{\nu})$ was performed.

The spectrum processing algorithm was analogous to that used in [31]. First, in experimentally recorded spectra, we passed from the time scale to the frequency scale. The frequency scale of tuning $\bar{\nu}$ was determined using the interferometer with a free spectral range of 0.012 cm^{-1} . The theoretical spectrum [33, 34] was constructed in accordance with expressions (15) and (16) with the experimentally established values of modulation amplitudes m_1 and m_2 . In contrast to [31], not one but two regions with frequencies of 7185 and 7466 cm^{-1} were fitted simultaneously. We assumed the Voigt type of the absorption line shapes. In each range, the fitting parameters were the positions of the absorption line centers and their Lorentz widths. The common fitting parameter in the two ranges was temperature T . As a consequence, the Voigt profiles were fitted with appropriate Doppler widths.

The fitting was performed by the nonlinear least squares method. As proposed in [13], the contribution from the first three orthogonal polynomials was subtracted from the experimental and simulated (fitting) spectra. From the analytical point of view, this is equivalent to fitting of the base line in expression (16) using a parabola [13].

The technique developed in this study was used for processing the results of a series of experiments on measuring different temperatures. For each temperature, three measurements were taken, and its average

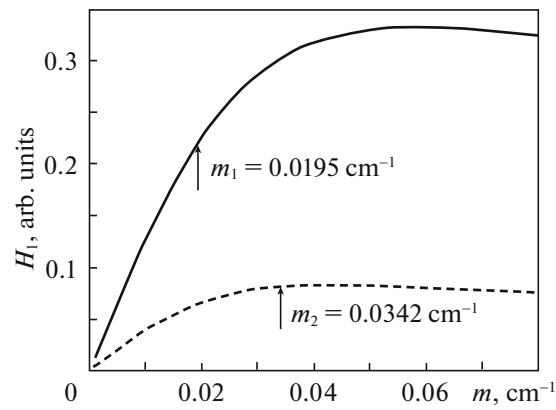


Fig. 4. Theoretical dependences of the amplitudes of the first ($1f$) harmonic of signal H_1 of the H_2O absorption line on modulation amplitude m_1 of the optical frequency for lines 7185.6 cm^{-1} (solid curve) and 7466.34 cm^{-1} (dashed curve) at a temperature of 1000 K ; m_1 and m_2 are the experimentally chosen values for lasers 7185 and 7466, respectively.

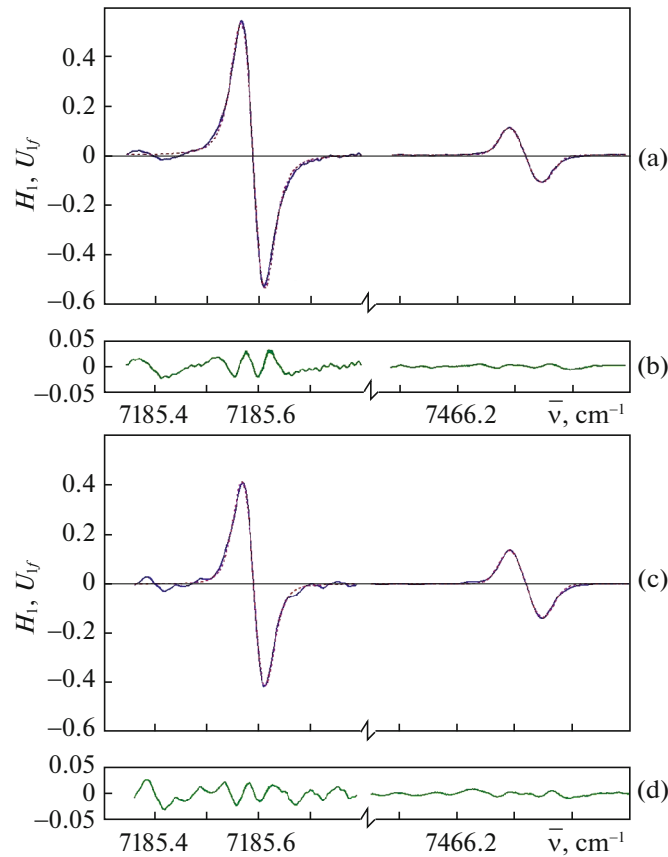


Fig. 5. Results of fitting of theoretical spectra H_1 (solid curves) to experimental spectra U_{1f} (dotted curves) for thermocouple readings $T = 826\text{ K}$ (a) and 1074 K (c) and residuals $\sigma = U_{1f} - H_1$ between experimental and model spectra (b, d).

value was determined. Temperature difference ΔT measured by a standard thermocouple and its mean value determined using this technique was 40 K for 1000 K and 30 K for 800 K .

For example, Fig. 5 shows the results of measurements and fitting of theoretical spectra for thermocouple readings of 826 and 1074 K . The temperatures obtained as a result of fitting were 828 and 1070 K , respectively.

5. CONCLUSIONS

In our investigations, we have demonstrated the effectiveness of our version of modulation spectroscopy DLAS (MS-DLAS) for determining the hot zone temperature. We have used the combination of slow (with frequency 122 Hz) tuning of laser radiation wavelengths in the vicinity of the water absorption lines and fast (with frequency ~ 50 kHz) modulation of wavelengths.

In the proposed MS-DLAS version of the method, we used the two-beam differential scheme with logarithmic conversion of experimental data and registration of the first harmonics of absorption signals of water molecules. The logarithmic conversion of signals and the two-beam differential scheme made it possible to substantially reduce the nonselective absorption of probe radiation and excessive laser noise.

Using the technique developed in this study, we have performed a series of experiments on measuring the temperature of air containing water vapor in the range 700–1100 K. Average deviation ΔT of the results of MS-DLAS and the readings of commercial thermocouples over the entire measuring cycle in the entire temperature range was 40 K.

The use of the first harmonic in the MS-DLAS method has a number of advantages. First, the (peak-to-peak) amplitude of the absorption signal at the first harmonic is approximately twice as large as at the second harmonic (and the more so, at higher harmonics), which increases the sensitivity of the sensor. Second, the registration of the second and higher harmonics of the absorption signal requires a broader band of the detecting system, which in turn requires the use of more costly sensor elemental base. In the case of simultaneous measurement at several wavelengths, one of the methods for separating the signals from two lasers is the modulation of the latter at different frequencies (multiplexing with separation in frequency) that differ from each other significantly. In this case, the use of the first harmonic makes it possible to lower the requirements to the detecting system. In addition, when the p - n junction is used as a logarithmic converter, nonlinearities increase with increasing frequency of the signal being detected, while nonlinearities for the first harmonic are minimal. Finally, the fitting of experimental spectra by the simulated theoretical spectrum of the first harmonic is much simpler than by spectra of normalized signals $2f/1f$, in which each term is the sum of intermodulated contributions to the Fourier expansion.

CONFLICT OF INTEREST

The authors declare that they have no conflicts of interest.

REFERENCES

1. Werle, P., A review of recent advances in semiconductor laser based gas monitors, *Spectrochim. Acta Part A.: Molec. Spectrosc.*, 1998, vol. 54, pp. 197–236.
[https://doi.org/10.1016/S1386-1425\(97\)00227-8](https://doi.org/10.1016/S1386-1425(97)00227-8)
2. Song, K. and Jung, E.C., Recent developments in modulation spectroscopy for trace gas detection using tunable diode lasers, *Appl. Spectrosc. Rev.*, 2003, vol. 38, pp. 395–432.
<https://doi.org/10.1081/ASR-120026329>
3. Lackner, M., Tunable diode laser absorption spectroscopy (TDLAS) in the process industries—A review, *Rev. Chem. Eng.*, 2007, vol. 23, p. 65.
<https://doi.org/10.1515/REVCE.2007.23.2.65>
4. Hodgkinson, J. and Tatam, R.P., Optical gas sensing: A review, *Meas. Sci. Technol.*, 2013, vol. 24, no. 1, p. 012004.
<https://doi.org/10.1088/0957-0233/24/1/012004>
5. Wang, F., Jia, S., Wang, Y., and Tang, Z., Recent developments in modulation spectroscopy for methane detection based on tunable diode laser, *Appl. Sci.*, 2019, vol. 9, p. 2816.
<https://doi.org/10.3390/app9142816>
6. Ponurovskii, Ya.Ya., New generation of gas-analytical systems, *Analytika*, 2019, vol. 9, p. 68.
7. Du, Z., Zhang, S., Li, J., Gao, N., and Tong, K., Mid-infrared tunable laser-based broadband fingerprint absorption spectroscopy for trace gas sensing: A review, *Appl. Sci.*, 2019, vol. 9, no. 2, p. 338.
<https://doi.org/10.3390/app9020338>
8. Fu, B., Zhang, C., Lyu, W., et al., Recent progress on laser absorption spectroscopy for determination of gaseous chemical species, *Appl. Spectrosc. Rev.*, 2022, vol. 57, pp. 112–152.
<https://doi.org/10.1080/05704928.2020.1857258>
9. Allen, M.G., Diode laser absorption sensors for gas-dynamic and combustion flows, *Meas. Sci. Technol.*, 1998, vol. 9, p. 545.
<https://doi.org/10.1088/0957-0233/9/4/001>

10. Bolshov, M.A., Kuritsyn, Yu.A., and Romanovskii, Yu.V., Tunable diode laser spectroscopy as a technique for combustion diagnostics, *Spectrochim. Acta Part B: At. Spectrosc.*, 2015, vol. 106, pp. 45–66.
<https://doi.org/10.1016/j.sab.2015.01.010>
11. Goldenstein, C.S., Spearrin, R.M., Jeffries, J.B., and Hanson, R.K., Infrared laser-absorption sensing for combustion gases, *Progr. Energy Combust. Sci.*, 2017, vol. 60, pp. 132–176.
<https://doi.org/10.1016/j.peccs.2016.12.002>
12. Liu, C. and Xu, L., Laser absorption spectroscopy for combustion diagnosis in reactive flows: A review, *Appl. Spectrosc. Rev.*, 2018, vol. 54, pp. 1–44.
<https://doi.org/10.1080/05704928.2018.1448854>
13. Liger, V.V., Mironenko, V.R., Kuritsin, Yu.A., and Bolshov, M.A., Diagnostics of hot zones by absorption spectroscopy method with diode lasers (review), *Opt. Spectrosc.*, 2019, vol. 127, pp. 49–60.
<https://doi.org/10.1134/S0030400X19070166>
14. Wang, J.Y., Laser absorption methods for simultaneous determination of temperature and species concentrations through a cross section of a radiating flow, *Appl. Opt.*, 1976, vol. 15, pp. 768–773.
<https://doi.org/10.1364/AO.15.000768>
15. Hanson, R.K. and Falcone, P.K., Temperature measurement technique for high-temperature gases using a tunable diode laser, *Appl. Opt.*, 1978, vol. 17, pp. 2477–2480.
<https://doi.org/10.1364/AO.17.002477>
16. Baer, D.S., Nagali, V., Furlong, E.R., Hanson, R.K., and Newfield, M.E., Scanned- and fixed-wavelength absorption diagnostics for combustion measurements using multiplexed diode lasers, *AIAA J.*, 1996, vol. 34, p. 489.
<https://doi.org/10.2514/3.13094>
17. Bolshov, M.A., Kuritsyn, Yu.A., Liger, V.V., Mironenko, V.R., Leonov, S.B., and Yarantsev, D.A., Measurements of gas parameters in plasma-assisted supersonic combustion processes using diode laser spectroscopy, *Quantum Electron.*, 2009, vol. 39, p. 869.
<https://doi.org/10.1070/QE2009v039n09ABEH014044>
18. Philippe, L.C. and Hanson, R.K., Laser diode wavelength-modulation spectroscopy for simultaneous measurement of temperature, pressure, and velocity in shock-heated oxygen flows, *Appl. Opt.*, 1993, vol. 32, no. 30, pp. 6090–6103.
<https://doi.org/10.1364/AO.32.006090>
19. Silver, J.A. and Kane, D.J., Diode laser measurements of concentration and temperature in microgravity combustion, *Meas. Sci. Technol.*, 1999, vol. 10, no. 10, p. 845.
<https://doi.org/10.1088/0957-0233/10/10/303>
20. Duffin, K., McGettrick, A.J., Johnstone, W., Stewart, G., and Moodie, D.G., Tunable diode-laser spectroscopy with wavelength modulation: A calibration-free approach to the recovery of absolute gas absorption line shapes, *J. Light. Technol.*, 2007, vol. 25, no. 10, pp. 3114–3125.
<https://doi.org/10.1109/JLT.2007.904937>
21. Rieker, G.B., Jeffries, J.B., and Hanson, R.K., Calibration-free wavelength-modulation spectroscopy for measurements of gas temperature and concentration in harsh environments, *Appl. Opt.*, 2009, vol. 48, pp. 5546–5560.
<https://doi.org/10.1364/AO.48.005546>
22. Lan L.J., Ding Y.J., Peng Z.M., Du Y.J., and Liu Y.F., Calibration-free wavelength modulation for gas sensing in tunable diode laser absorption spectroscopy, *Appl. Phys. B*, 2014, vol. 117, pp. 1211–1219.
<https://doi.org/10.1007/s00340-014-5945-4>
23. Goldenstein, C.S., Strand, C.L., Schultz, I., Sun, K., and Jeffries, J.B., Hanson, R.K., Fitting of calibration-free scanned-wavelength-modulation spectroscopy spectra for determination of gas properties and absorption lineshapes, *Appl. Opt.*, 2014, vol. 53, pp. 356–367.
<https://doi.org/10.1364/AO.53.000356>
24. Liger, V.V., Kuritsyn, Yu.A., Krivitsun, V.M., Snegirev, E.P., and Kononov, A.N., Measurement of the absorption with a diode laser characterised by a detection threshold governed by the shot noise of its radiation, *Quantum Electron.*, 1997, vol. 27, no. 4, p. 360.
<https://doi.org/10.1070/QE1997v027n04ABEH000949>
25. Liger, V., Zybin, A., Kuritsyn, Y., and Niemax, K., Diode-laser atomic-absorption spectrometry by the double-beam—double-modulation technique, *Spectrochim. Acta Part B: At. Spectrosc.*, 1997, vol. 52, no. 8, pp. 1125–1138.
[https://doi.org/10.1016/S0584-8547\(97\)00029-3](https://doi.org/10.1016/S0584-8547(97)00029-3)
26. Zybin, A.V., Liger, V.V., and Kuritsyn, Yu.A., Dynamic range improvement and background correction in diode laser atomic absorption spectrometry, *Spectrochim. Acta Part B: At. Spectrosc.*, 1999, vol. 54, pp. 613–619.
[https://doi.org/10.1016/S0584-8547\(98\)00230-4](https://doi.org/10.1016/S0584-8547(98)00230-4)
27. Wang, Y., Cai, H., Geng, J., and Fang, Z., Logarithmic conversion of absorption detection in wavelength modulation spectroscopy with a current-modulated diode laser, *Appl. Opt.*, 2009, vol. 48, pp. 4068–4076.
<https://doi.org/10.1364/AO.48.004068>

28. Cong, M. and Sun, D., Detection of ammonia using logarithmic-transformed wavelength modulation spectrum, *IOP Conf. Ser. Mater. Sci. Eng.*, 2018, vol. 381, p. 012132.
<https://doi.org/10.1088/1757-899X/381/1/012132>
29. Li, S. and Sun, L., Natural logarithm wavelength modulation spectroscopy, *Chinese Opt. Lett.*, 2021, vol. 19, p. 031201.
<https://doi.org/10.1364/COL.19.031201>
30. Li, R., Li, F., Lin, X., and Yu, X., Linear calibration-free wavelength modulation spectroscopy, *Microw. Opt. Technol. Lett.*, 2023, vol. 65, no. 5, pp. 1024–1030.
<https://doi.org/10.1002/mop.33063>
31. Liger, V., Mironenko, V., Kuritsyn, Yu., and Bolshov, M., Advanced fiber-coupled diode laser sensor for calibration-free 1f-WMS determination of an absorption line intensity, *Sensors*, 2020, vol. 20, no. 21, p. 6826.
<https://doi.org/10.3390/s20216286>
32. Bolshov, M.A., Kuritsyn, Yu.A., Liger, V.V., and Mironenko V.R., Development of diode laser absorption spectroscopy method for determining temperature and concentration of molecules in remote object, *Opt. Spectrosc.*, 2011, vol. 110, pp. 848–856.
<https://doi.org/10.1134/S0030400X1106004X>
33. Gordon, I.E., et al., The HITRAN2016 molecular spectroscopic database, *J. Quant. Spectrosc. Radiat. Transf.*, 2017, vol. 203, pp. 3–69.
<https://doi.org/10.1016/j.jqsrt.2017.06.038>
34. Rothman, L.S. et al., HITEMP, the high-temperature molecular spectroscopic database, *J. Quant. Spectrosc. Radiat. Transf.*, 2010, vol. 111, pp. 2139–2150.
<https://doi.org/10.1016/j.jqsrt.2010.05.001>

Translated by N. Wadhwa